Original Paper

Indoor and Built Environment

Indoor and Built Environment
2015, Vol. 24(1) 11–26

DOI: 10.1177/1420326X13500294
ibe.sagepub.com

SAGE

A review of membrane-based air dehumidification

Bo Yang[1], Weixing Yuan[1], Feng Gao[2] and Binghan Guo[1]

Abstract

Air dehumidification plays an important role in improving air quality and maintaining thermal comfort. Increasing attention is paid to the membrane-based technology, which is based on water vapour transmembrane transport driven by mass transfer potential, together with sensible heat transfer under temperature difference. Membrane-based air dehumidification has been applied in heating, ventilation and air conditioning, compressed air dehumidification and environmental control in space vehicle, and some other engineering fields. This paper summarizes recent research results in these fields, including fundamental principles, membrane materials, membrane module structures, operation conditions and theory models. In the end, two methods of membrane-based dehumidification performance evaluation are introduced from perspective of energy and exergy, respectively.

Keywords

Dehumidification, Membrane, Mass transfer, Heat transfer, Evaluation

Accepted: 12 July 2013

Introduction

Humidity is an important parameter that can affect thermal comfort.[1] High humidity will not only lead to discomfort and influence the body surface temperature, but also benefit germs breeding, which gives rise to many health problems such as SARS and H1N1.[2,3] The ASHRAE Standard 62-2001 recommends the relative humidity of 30–60% for indoor environment.[4] In some special circumstances such as machine room, museum and library, high humidity needs to be avoided.

In some hot and humid regions such as Southern China where outside air humidity stays above 80–90% continuously for a dozen of days,[5] latent heat load caused by fresh ventilation air of high humidity can account for 20–40% of the total energy consumption of heating, ventilation and air conditioning (HVAC) system.[3] Obviously, effective dehumidification for fresh air would be of great importance in energy saving and reduction of carbon emission. It is shown that building energy consumption could be reduced by 20–64% by using efficient dehumidification technologies.[6]

As can be seen, air dehumidification can play more and more important role in energy saving. Considering dehumidification efficiency and special applications for further, membrane-based dehumidification stands out from various dehumidification technologies, for its simple structure without rotary parts, non-direct contacting of air with working substance, continuously working mode, reliability, high dehumidification efficiency and so on.[7,8] Due to these advantages, membrane-based air dehumidification is being studied extensively and even being taken into practical applications, including total heat recovery in HVAC,[9] compressed air dehumidification,[10] space application,[11] etc.

Membrane-based dehumidification in field of HVAC

In air conditioning, fresh air is usually ventilated into room to guarantee indoor air quality (IAQ). However,

[1]Laboratory of Ergonomics and Environmental Control, School of Aeronautic Science and Engineering, Beihang University, Beijing, China
[2]Chinese Astronaut Training Center of Scientific Research, Beijing, China

Corresponding author:
Weixing Yuan, Laboratory of Ergonomics and Environmental Control, School of Aeronautic Science and Engineering, Beihang University, Beijing, China.
Email: yuanwx@buaa.edu.cn

as mentioned above, high humidity of fresh air not only brings discomfort, but also adds heat load to HVAC system. Dehumidification for fresh air before cooling is thereby necessary. Traditional dehumidification technology consumes much energy, such as heat-driven dehumidification by desiccant and common dew point dehumidification. On the other hand, additional parts designed for dehumidification also add the complexity of system as well. However, liquid desiccant and dew point methods have some limitations, especially the fouling and hygiene problems. Therefore, membrane method is proposed as a new type of dehumidification technology. In the novel HVAC system, fresh air is cooled by chilled ceiling[12] or by evaporator of compression refrigeration system,[13,14] after exchanging the total heat with exhaust air[13,14] or liquid desiccant.[15,16] There are abundant investigations on membrane-based dehumidification applied in HVAC, with topics from fundamental principles, materials, structures and operation conditions to theory models. Zhang summarized the work of his team over the past 10 years covering almost all aspects of total heat recovery with membranes applied in HVAC from fundamentals to engineering applications.[17] Combining a refrigeration fresh air unit with the developed membrane-based total heat exchanger, the novel system obtained a COP as high as 5.8. Compared with this, the COPs of the traditional common systems were usually below 2.8.

Fundamental principles

Membrane-based dehumidification is based on moisture transfer driven by mass transfer potential difference between membrane's two sides called feed side and permeate side, respectively. In HVAC system, the mass transfer potential mainly comes from water vapour partial pressure difference (also humidity ratio difference). Mass transfer flux, J (kg s^{-1}) is defined by equation (1):

$$J = k\Delta\omega A \tag{1}$$

where k is mass transfer coefficient (kg m^{-2} s^{-1}); $\Delta\omega$ is humidity ratio difference (kg kg^{-1} dry air) and A is membrane surface area (m^2). Sometimes moisture transfer flux is represented as volumetric flow rate (m^3 s^{-1}) where k is in m s^{-1}.

The relative humidity of air is calculated by humidity ratio and temperature by equation (2),[18] as

$$\frac{\varphi}{\omega} = \frac{e^{5294/T}}{10^6} - 1.61\varphi \tag{2}$$

where T is in K and φ is relative humidity. In general, the second term on the right-hand side can be neglected.

In particular, since a saturated thin layer exists on the surface of water, the humidity ratio of water can be formulated in the humidity ratio of saturated humid air:[9]

$$\omega_w = \frac{10^6}{e^{5294/T}} \tag{3}$$

Similarly, the humidity ratio of solution can be calculated by

$$\omega_s = \frac{\chi 10^6}{e^{5294/T}} \tag{4}$$

where χ is the concentration of water.

Materials

Selectivity and permeability are two significant performance characteristics of material used for membrane-based air dehumidification. Selectivity means that only vapour can transfer through membrane while air is obstructed outside, consequently realizing separation. However, absolute separation is impossible, since air can also get through membrane pores to some extent, although the proportion is very small versus vapour. For this reason, porous hydrophilic membrane is usually applied to air dehumidification, such as polyvinyl alcohol (PVA), celluloid, cellulose acetate (CA) and polyimide (PI).[19] Generally speaking, the higher the porosity of membrane is, the faster the vapour transfers and therefore the higher the permeability will be. In addition, hydrophilicity of membrane material also benefits vapour permeation, which may be more influential in some degree.

Membrane materials applied to dehumidification includes organics (polymers mainly, more commonly used) and inorganics such as silicate. Since nitrogen accounts for the main component of air, H_2O/N_2 separation properties determine air dehumidification performance to a great extent. Table 1 gives water vapour permeabilities and H_2O/N_2 selectivities at 30°C for various organic polymers.[20]

As shown in Table 1, there are very few membranes combining high water vapour permeability with high H_2O/N_2 selectivity, such as PEBAX® 1074 and sulphonated poly (ether ether ketone). For most membranes, unfortunately, high water vapour permeability and high H_2O/N_2 selectivity cannot be obtained at the same time. For instance, PI and polyacrylonitrile have extremely high H_2O/N_2 selectivities of 5,330,000 and 1,880,000, respectively, with quite low water vapour permeabilities of 4.86×10^{-15} m^2 s^{-1} Pa^{-1} and 2.28×10^{-15} m^2 s^{-1} Pa^{-1}, respectively . Moreover, for some other membranes such as polypropylene and polyethylene, both permeability and selectivity are very low.

Table 1. Water vapour permeabilities and H_2O/N_2 selectivities at 30°C for various organic polymers.[20]

Polymer	Water vapour permeability, 10^{-18} m^2 s^{-1} Pa^{-1}	Selectivity, H_2O/N_2
PEBAX® 1074[a]	1,216,000	200,000
PBT/PEO block copolymer[b]	649,800	40,500
Sulphonated poly (ether ether ketone)	463,600	10,200,000
Polydimethylsiloxane	304,000	143
Sulphonated poly (ether sulphone)	114,000	214,000
Ethyl cellulose	152,000	6060
Cellulose acetate	45,600	24,000
Poly (phenylene oxide)	30,856	1068
Poly (ether sulphone)	19,912	10,500
Natural rubber	19,760	299
Polysulphone	15,200	8000
Polycarbonate	10,640	4670
Polystyrene	7372	388
Polyimide	4860	5,330,000
Polyacrylonitrile	2280	1,880,000
Poly (vinyl chloride)	2090	12,500
Polyamide 6	2090	11,000
Polypropylene	517	227
Poly (vinyl alcohol)	144	33,300
Polyethylene	91	6

[a]PEBAX® 1074 is a blend of polyether block amide (nylon12) and poly (ethylene oxide).
[b](Polybutylene terephthalate)/poly (ethylene oxide) copolymer.

Permeability and selectivity are incompatible with each other for most membranes of simple structure and property. Therefore, membrane module is usually fabricated with composite membranes, or taken modification technology. Sometimes the two technologies are utilized together. To fabricate composite membrane, an active layer is sedimentated as a skin layer on the surface of a support layer. The high hydrophilic skin layer made from dense membrane or liquid membrane has a greater mass transfer resistance and is therefore manufactured thinner than the support layer which primarily contributes to enhancement on mechanical strength.

A green method of one-step fabrication of an asymmetric CA membrane was introduced in the literature.[21] CA, acetic acid and de-ionized water of specific weight ratios were prepared. After some treatment of mixing, cooling, slicing, immersing in tap water twice and then drying in vacuum oven, an asymmetric membrane with a dense layer on the surface was formed. It was found that the surface was denser with an increase of de-ionized water in the casting solution.

The mass transfer performance of an asymmetric membrane was studied.[22] The thickness of the dense layer accounted for only 1/10 of the total thickness, while mass transfer resistance accounted for more than 50%. The remaining resistance of less than 50% was equally accounted for by convective mass transfer resistance of the boundary layers of both sides and diffusion resistance of the support layer. It was shown that asymmetric membrane had better moisture transfer capacity with respect to traditional paper membrane. Porous structure conduces to moisture permeation, but plain porous membrane usually cannot be directly applied to dehumidification yet for its relatively low vapour permeability, in the order of 10^{-12}–10^{-13} m^2 s^{-1} (it should be noted that the driven force of permeation here is considered as humidity difference, hence the unit of vapour permeability is m^2 s^{-1}), compared with 10^{-9} m^2 s^{-1} of liquid membrane.[23] Considering this, simple structured membrane is usually modified by depositing hydrophilic material such as quaternary ammonium salt or halide salt into membrane pores.

An LiCl solution-based composite supported liquid membrane (CSLM) was successfully fabricated.[24] The liquid LiCl solution was immobilized into the macro and micro pores of porous support CA membrane, while two hydrophilic polyvinylidene fluoride (PVDF) membranes were formed on both surfaces as skin layers. It was observed that the moisture permeation rate through the CSLM was two times higher than that through the solid membrane.

Silicate membrane Al-MCM-48 was studied on H_2O/O_2 separation process to compare with MCM-48.[25] The α-Al membrane was used as support with pore diameter of 0.2 μm and thickness of 2 mm. The thickness of skin layer was 25 μm and 45 μm for MCM-48 and Al-MCM-48, respectively, as shown in Figure 1. Since the addition of aluminium has promoted dissolution of polar water molecule, Al-MCM-48 would provide better hydrophilicity.

PVA solution was blended with LiCl to fabricate dense membrane, while porous polythersulphone was used as support.[26] The composite membrane had a smaller contact angle when immersed in water, gaining better hydrophilicity; as a consequence the moisture permeation got facilitated. In addition, the membrane became more flexible and mechanically robust due to a decrease in crystallinity.

Liquid may immerse in pores and destroy inner structure when contacting membrane directly, so it is necessary to apply hydrophobization on the permeate side, or composite with a layer of hydrophobic membrane. This would benefit moisture removal, thus preventing concentration polarization. PVDF is a typical hydrophobic material applied to dehumidification, on which some hydrophilic materials such as PVA and

polyethylene glycol are usually modified to form a hydrophilic–hydrophobic composite membrane.[27–30]

A PVDF membrane was modified with a dense layer made from α,β-dihydroxy polydimethylsiloxane.[31] Though vapour permeability decreased slightly, the contact angle on the permeate side could be modified with hydrophobization by increasing to 120° from 60°, which effectively would prevent liquid leaking towards the feed side.

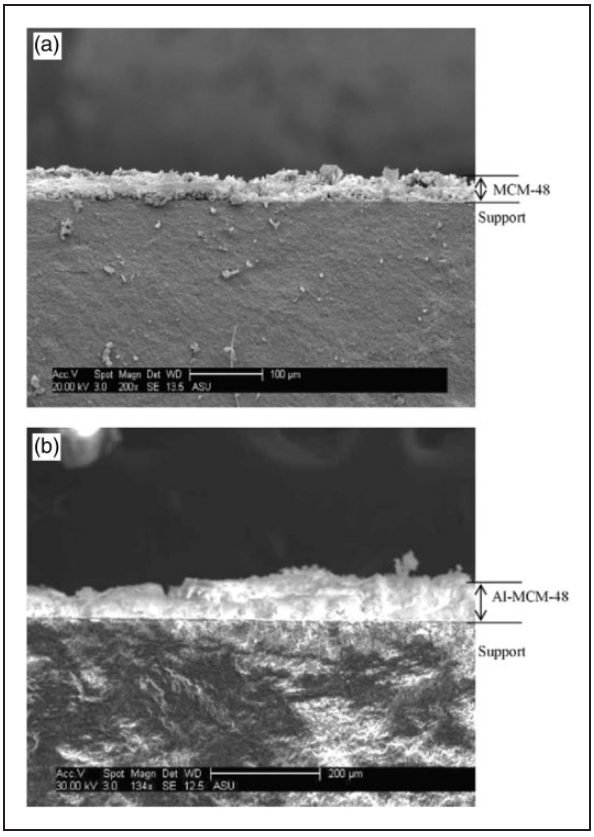

Figure 1. SEM micrograph of (a) MCM-48 membrane and (b) Al-MCM-48 membrane.[25]
SEM: scanning electron microscope.

What has been discussed above is mainly on the separation of water vapour from oxygen or nitrogen, and surely it is a preliminary demand for dehumidification anyhow. However, besides moisture and the major components of air, volatile organic compounds (VOCs) may enter the fresh air from the exhaust air through membrane pores as well. For the sake of IAQ, membrane material should be a great barrier to VOCs.[32] From the comprehensive perspective, PVA-1 (PVA with LiCl as an additive) is the best material with a high moisture permeability of 3.7×10^{-8} m^2 s^{-1} and a high water vapour selectivity with respect to VOCs (360, 333, 340, 451 and 333 for acetic acid, formaldehyde, acetaldehyde, toluene and ethane, respectively).[33] As for airborne bacterial, Ag^+ is alternative for its sterilization ability, which can be coated on the membrane surface.[34]

Structures

Similar to conventional sensible heat exchanger, there are mainly two forms for membrane module, shell-and-tube type[35–37] and plate type.[38,39]

Shell-and-tube membrane module is fabricated with a bundle of hollow fibres packed inside shell, obtaining very excellent specific area even as high as 2000 m^2 m^{-3}. Feed air flows at the tube side, or shell side. Figure 2 shows a type of counter flow hollow fibre membrane dehumidifier, with feed air flowing at the shell side and LiCl at the tube side, whose packing fraction is 0.25, and specific area is 750 m^2 m^{-3}.[40]

With the same structure as conventional metal shell-and-tube heat exchanger, hollow fibre membrane module exhibits extremely different features, however, including much smaller characteristic diameters and much larger number of fibres. As a result, the flow tends to be turbulent even at much lower Reynolds numbers. The κ–ω model was found to fit the experiments well where *Re* ranged from 100 to 300, while the laminar model only fitted the tests well at *Re* below 150.[41] In addition, packing density is a dominant

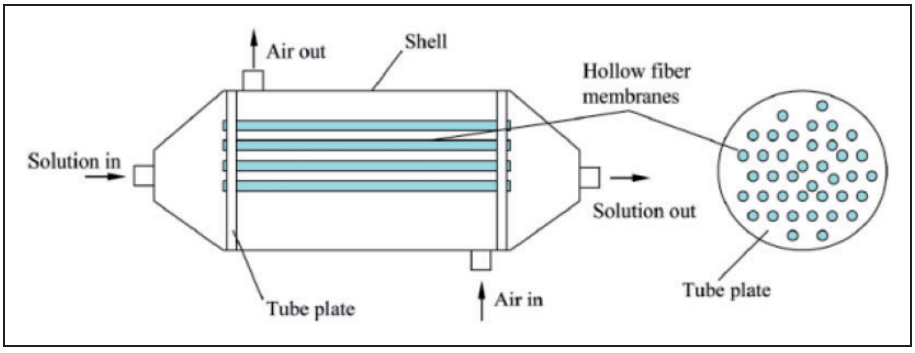

Figure 2. A type of hollow fibre membrane module.[40]

factor for performance in membrane module, while the impact of flow arrangement is quite little. In contrary to this, flow arrangement plays an important role in sensible heat exchanger.[42]

Flat plate is another common type due to its simple structure. Feed air and permeate fluid flow staggeredly between adjacent plates. Figure 3 presents the structure of a quasi-counter membrane dehumidifier.[43] The flat-plate total heat exchanger exhibits quite different heat transfer performances from the traditional ones. Due to the combination of heat and mass transfer, it was found that the Nusselt numbers calculated by real boundary condition deviated largely from those by uniform wall temperature condition and uniform wall heat flux condition under low aspect ratios.[44]

Besides flat-plate type, membrane module can be made in the form of plate-fin type as well. As a result of lower fin conductance parameter (a dimensionless number representing the heat conductivity of the fins with respect to that of the fluid), the heat transfer performances in plate-fin membrane exchanger indicate a great difference from those in conventional metal-fin sensible heat exchanger.[45] In metal-fin ducts, both plates and fins contribute to the heat transfer to/from the fluid, while the heat is mainly transferred through the plates in polymer-fin ducts, leading to a slower heat exchange between the plates and the bulk fluid and obtaining lower fin efficiencies and Nusselt numbers therefore.[46,47]

A novel membrane module was proposed which used CSLMs as transfer plates with addition of paper membrane fins. The latent efficiency of the novel module was 60% higher than the total paper membrane module.[48]

Just like the traditional sensible heat exchanger, the basic flow configuration of membrane module includes current, counter and cross flows. The actual membrane module may combine current with cross or counter with cross. In the counter flow, two headers would need to be placed side by side at the inlet and outlet, while the counter–cross flow configuration avoids such header complexity by placing the inlet and outlet headers of the two fluids on the top and bottom of the module.[6] It was predicted[49] that a small entrance ratio (ratio of liquid entrance length to exchanger length) and exchanger aspect ratio (ratio of membrane height to exchanger length) of the counter–cross flow could always result in a better performance than the cross flow with the same membrane surface area.

Combining cross-flow configuration with triangular ducts, the cross-corrugated structure provides high mass transfer capacities, due to the strong swirls generated in the lower troughs that intensify the momentum and mass transfer, as shown in Figure 4.[50,51] It was observed that the corrugation angle of 90° could obtain the greatest mass transfer improvement compared with 0° and 45°.[52] As a result of the complex duct structure, conventional laminar correlations could not predict the flow with low Reynolds number any more. Low Reynolds number κ–ω model was validated to fit the experiment results well in the Re range of 100–3000[50] and 500–5000,[53] respectively, for different duct sizes.

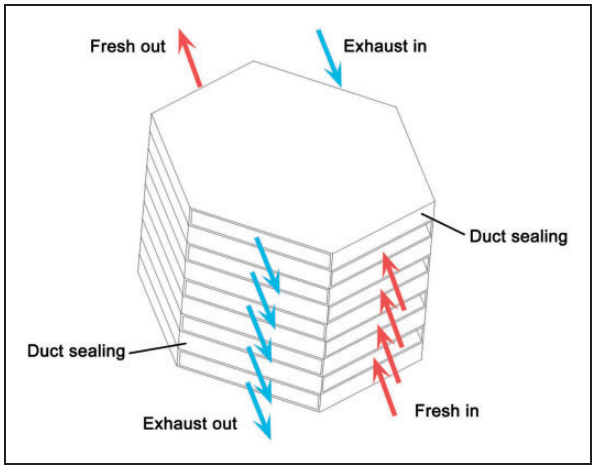

Figure 3. A type of quasi-counter plate membrane module.[43]

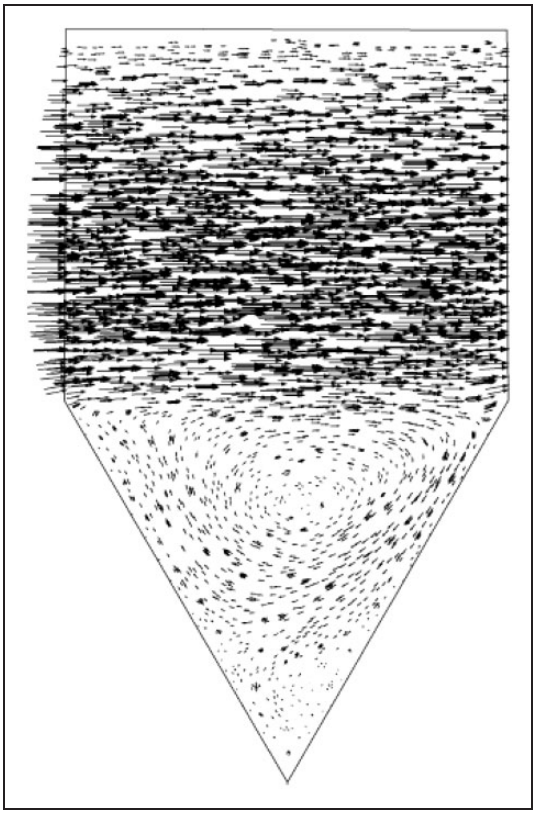

Figure 4. Velocity vectors in cross-corrugated duct at $Re = 1500$.[50]

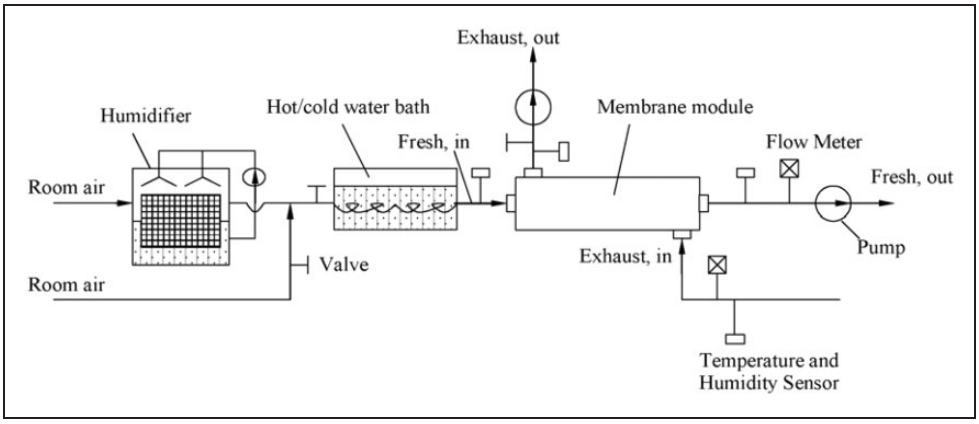

Figure 5. An experimental setup for membrane module heat and moisture recovery.[37]

A wider transitional flow range of *Re* at 100–6000 was studied using low Reynolds number κ–ω model as well.[54] As for turbulent flow ($2000 < Re < 20{,}000$), Reynolds stress model gave the best prediction.[55]

Recently, the flow maldistribution problem has drawn much attention, which universally exists for various structures and brings significant performance deterioration. It may be caused by the complex structures such as irregular fibre packing, non-uniform arrangement, large channel pitch and tortuous inlet header.[56–60] Generally, there exists more serious flow maldistribution for the flat-plate structure compared to the plate-fin structure.

Operation conditions

During dehumidification process, water vapour from fresh air permeates through membrane pores and reaches the other side. Water molecules accumulate in the surface pores of the permeate side, restrained by capillary force, leading to a decrease in mass transfer potential. So there is a need to build in some mechanism to remove effectively to get a better performance. In HVAC system, indoor exhaust air usually performs as working fluid of the permeate side.

A hollow fibre membrane module was tested in an air-conditioned room.[37] Room air was first humidified and heated in a hot/cool water bath, then exchanged heat and moisture with the exhaust air flow directly driven from room, as shown in Figure 5. Various inlet conditions of mass flow rate, temperature and humidity were tested to observe the effects on dehumidification performance.

In addition to low humidity air, liquid is also usually used as dehumidification fluid. Owing to the high absorption capacity per unit mass of liquid phase, very low liquid velocity can be adopted, resulting in low pressure loss along the membrane module.[61]

Different from air-to-air mode in which the air of the permeate side is exhausted, air-to-solution mode adopts a circulation loop for the solution. As dehumidification is processing, the solution temperature increases, and concentration drops, subsequently the mass transfer potential decreases. Considering that the exhaust air is relatively hot and dry compared with the diluted solution, another membrane module can be used to recover the sensible and latent heat of solution to keep the dehumidification proceeding,[6,8] as shown in Figure 6.

A hollow fibre membrane module was experimentally investigated using a saturated LiCl solution flowing in tubes, with air flowing in shell by cross flow.[62] Experimental results indicated that the mass flow rate of LiCl solution affected dehumidification effectiveness little, while an increase in air flow rate brought about a slight decrease in effectiveness.

Benefiting from the high absorption capacity, liquid desiccant is commonly applied to membrane total heat exchanger in vapour compression refrigeration and dehumidification hybrid system. In the hybrid system, the liquid desiccant is initially cooled by evaporator, and then it takes away the sensible and latent heat of fresh air simultaneously through the membrane exchanger. The diluted desiccant is regenerated by the combination of condenser and another membrane exchanger to maintain the absorption capacity.[15,16]

Theoretically, as long as the permeate side can offer a relatively low water vapour partial pressure atmosphere, dehumidification would be possible. Cooled pure water is thus an alternative working fluid for the permeate side, especially for its non-corrosivity and low price relative to solution.[8]

Theory models

During membrane-based dehumidification process, heat and mass transfer proceed simultaneously.

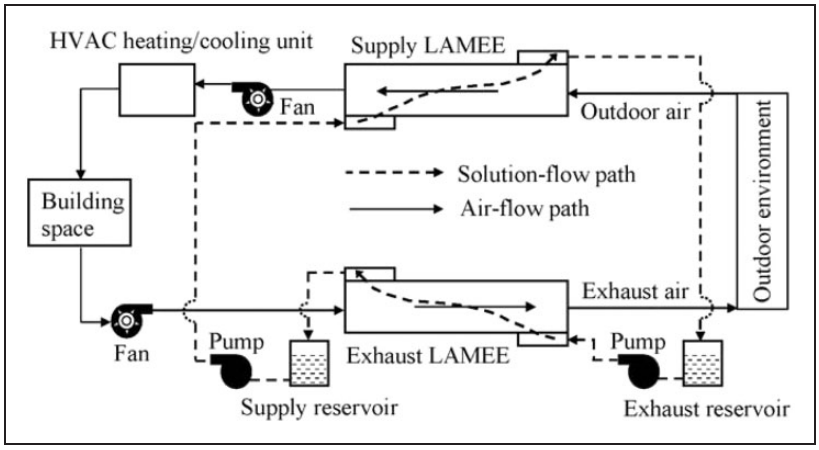

Figure 6. Schematic of a run-around membrane energy exchanger system in HVAC line.[6]
HVAC: heating, ventilation and air conditioning.

Heat is transferred by conductivity across membrane and convection of fluid, forming linear temperature distribution across membrane and temperature boundary layers on the surfaces.[63,64] The humidity distribution is similar, as shown in Figure 7.

Diffusion in membrane

Seshadri and Lin[25] identified transfer mechanism of gas in membrane as activated diffusion, Knudsen diffusion and viscous flow, dominating in microporous ($d_p <$ 2 nm), mesoporous (2 nm $< d_p <$ 50 nm) and macroporous ($d_p >$ 50 nm) membrane, successively. Theoretically, the best separation factor can be gained when Knudsen diffusion is the governing mechanism as represented by equation (5). In this mechanism, permeability is inversely proportional to square roots of the molecule weight

$$D_k = \frac{d_p}{3}\sqrt{\frac{8RT}{\pi M_v}} \tag{5}$$

where d_p is mean diameter of pores (m); R is gas constant, 8.314 J mol^{-1} K^{-1} and M_v is the molecule weight of vapour (kg mol^{-1}).

Zhang[23] considered the transfer mechanism in most microporous membrane as combination of Knudsen and molecule diffusion.[23] The molecular diffusivity of water vapour in air is given by equation (6)

$$D_o = \frac{C_a T^{1.75}}{P_m\left(v_v^{1/3} + v_a^{1/3}\right)^2}\sqrt{\frac{1}{M_v} + \frac{1}{M_a}} \tag{6}$$

where $C_a = 3.203 \times 10^{-4}$; $v_v = 20.1$; $v_a = 12.7$; P_m is mean pressure in membrane pores (Pa) and M_v and M_a are molecule weights of vapour and air, respectively. Overall diffusivity is defined by equation (7)

$$D_{vm} = \left(D_k^{-1} + D_o^{-1}\right)^{-1} \tag{7}$$

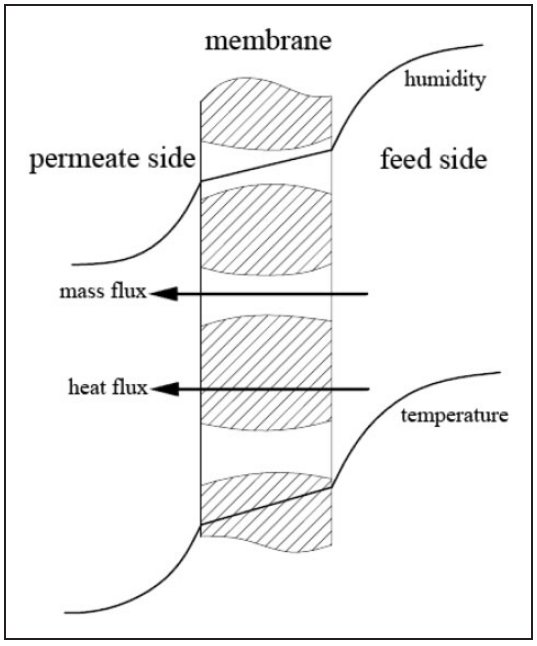

Figure 7. Distribution of temperature and humidity inside the membrane and on the surfaces.

Another diffusion mechanism in dense membrane is capillary condensation. Under this mechanism, water vapour is absorbed by membrane surface, then condensates in membrane pores at a relatively lower pressure and blocks the flow of air consequently, resulting in higher selectivity than Knudsen diffusion.[25] The latent heat released by water vapour condensation transfers

towards the other side under the temperature difference, conferring the system the evaporation energy while water leaves the membrane pores at vapour state.[32] To establish mathematical models easily, this process is sometimes simplified so that no phase change occurs in air-to-air mode[37] and only condensation occurs at the liquid–membrane interface in air-to-liquid mode.[62]

Convective transfer in boundary layers

The same heat transfer correlation can be used for flow both between plates and in tube. For laminar flow, Hausen is commonly used to calculate the Nusselt number[65] as represented by equation (8)

$$Nu = 3.658 + \frac{0.085[RePr(d_h/L)]}{1 + 0.047[RePr(d_h/L)]^{0.67}}\left(\frac{\mu_f}{\mu_w}\right)^{0.14} \quad (8)$$

where d_h is hydrodynamic diameter (m); L is membrane length (m); μ_f and μ_w are dynamic viscosity (Pa s) specified by temperature of fluid and wall, respectively and Re, Pr and Nu denote Reynolds, Prandtl and Nusselt numbers, respectively. It should be noted that equation (8) applies to $RePr(d_h/L) < 100$.

When $RePr(d_h/L)$ is greater, Sieder–Tate is applicable[65]

$$Nu = 1.86[RePr(d_h/L)]^{0.33}\left(\frac{\mu_f}{\mu_w}\right)^{0.14} \quad (9)$$

For turbulent flow, Dittus–Boelter will be applied[65]

$$Nu = 0.023Re^{0.8}Pr^n \quad (10)$$

where n equals 0.4 when fluid is heated and 0.3 when cooled.

For the shell side of hollow fibre membrane, if fluid flows along axis of tube, the Nusselt number can be obtained by correlation for flow in tube, with hydrodynamic diameter calculated by flow area and wet perimeter of the shell side. If fluid flows perpendicularly to tube, Zukauskas is used[66]

$$Nu = CRe^mPr^n\left(\frac{Pr}{Pr_w}\right)^{0.25}Fc \quad (11)$$

where Pr_w is the Prandtl number specified by temperature of wall and C, m, n and Fc can be obtained referring to charts and figures.[66]

Many literature works give the similar form of mass transfer correlation of the shell side as equation (12) as follows[67–70]

$$Sh = CRe^mSc^n \quad (12)$$

where C is a function of hydrodynamic diameter, length and packing density (m^2 m^{-3}) and Sc and Sh are Schmidt and Sherwood numbers. However, these correlations are just applicable in specific void fraction or packing fraction, ϕ, and the Reynolds number, see equations (14) and (15). Among these correlations, the correlation by Lipnizki and Field[36] as represented by equations (13) to (16) is applicable to relatively wider conditions.

$$Sh = \left(Sh_1^3 + Sh_2^3 + Sh_3^3\right)^{1/3} \quad (13)$$

where

$$Sh_1 = 3.66 + 1.2\phi^{-0.4} \quad (14)$$

$$Sh_2 = 1.615(1 + 0.14\phi)^3(ReScd_h/L)^{0.5} \quad (15)$$

$$Sh_3 = \left(\frac{2}{1 + 22Sc}\right)^{1/6}(ReScd_h/L)^{0.5} \quad (16)$$

are the Sherwood numbers for hydrodynamic and concentration developed flow, hydrodynamic developed only and both developing, respectively.[36]

The Sherwood number of flow between plates or in tube that can be calculated by Chilton–Colburn analogy[37] is represented by equation (17) as

$$Sh = NuLe^{-1/3} \quad (17)$$

where $Le = Pr/Sc$ is the Lewis number.

The correlation below can also be used to calculate the Sherwood number of flow in tube by equation (18)[71]

$$Sh = 1.62(ReScd_h/L)^{0.33} \quad (18)$$

Convective heat and mass transfer coefficients in boundary layers are calculated by equations (19) and (20) as follows:

$$Nu = \frac{hd_h}{\lambda} \quad (19)$$

$$Sh = \frac{kd_h}{D} \quad (20)$$

where h is heat transfer coefficient (W m^{-2} K^{-1}); λ is heat conductivity of fluid (W m^{-1} K^{-1}) and D is diffusivity of water vapour in air or water in liquid (m^2 s^{-1}).

Then the total heat and mass transfer can be obtained by equations (21) and (22):

$$\frac{1}{h} = \frac{1}{h_1} + \frac{\delta}{\lambda_m} + \frac{1}{h_2} \quad (21)$$

$$\frac{1}{k}=\frac{1}{k_1}+\frac{\delta}{D_{vm}}+\frac{1}{k_2} \tag{22}$$

where λ_m is heat conductivity of membrane (W m^{-1} K^{-1}); D_{vm} is diffusivity of vapour in membrane (m^2 s^{-1}); δ is membrane thickness (m) and subscripts '1' and '2' denote the two sides of membrane, respectively.

Since the diffusion flux in membrane is equal to the overall transmembrane transfer flux, the isothermal sorption curve of membrane can be used to calculate the transfer flux instead of resolving the convective mass transfer coefficient.[72,73] The isothermal sorption curve can be obtained by humidification experiment

$$\theta=\frac{W_{\max}}{1-C+C/\varphi} \tag{23}$$

where θ of equation (23) is the water content of membrane (kg kg^{-1}); $W_{\max}$ is the maximum water content of membrane corresponding to $\varphi=1$; C is a constant and φ is the relative humidity of air. Thus

$$J=D_{vm}\frac{\theta_{m1}-\theta_{m2}}{\delta} \tag{24}$$

where θ_{m1} and θ_{m2} are the water contents of membrane at both surfaces. It should be noted that this methodology applies to hydrophilic membrane only, rather than hydrophobic one.[74] In fact, water content in hydrophilic media can be represented by the function of water vapour partial pressure on the surface. Since it is well known of the relation between water vapour partial pressure and humidity ratio, the two methodologies reach a unity in the end.[75]

Solution

The solution to heat and mass transfer process is obtained by numerical approach. By establishing mass, momentum, energy and component governing equations, various parameters including temperature, humidity and velocity can be solved simultaneously. Usually it is simplified that (1) the process is one-dimensional; (2) both of the two flows are uniform; (3) mass change in either flow caused by moisture transfer can be neglected and (4) heat and mass diffusion along axial direction are negligible. By simplification, mass and momentum equations can be omitted, leaving only energy and component equations to solve.

As sometimes more details are preferred, completed governing equations need to be established.[76] A free surface model approach was used to investigate the three-dimensional heat and mass transfer process in a hollow fibre membrane module.[77] In the fibre cell, liquid flowed in tube, while air flowed in annular channel surrounded by outer wall of tube and the free surface, as shown in Figure 8. Entry section effect was observed, with quite high values of Nusselt number and Sherwood number in entry regions. In addition, with momentum equation solved together, the velocity field was also obtained.

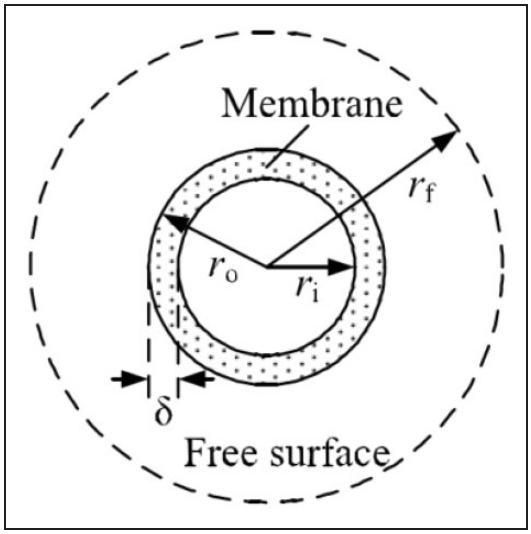

Figure 8. The fibre cell with a free surface.[77]

As mentioned fragmentarily above, the transport data in membrane module display a tremendous difference from that in sensible heat exchanger, as a result of the special structures and the conjugate heat and mass transfer boundary conditions. Especially for the flow regime classification according to Reynolds number, the turbulent flow occurs at much lower Reynolds number compared with classical data. On the other hand, either uniform wall temperature or uniform wall heat flux boundary condition only applies to some specific situations of packing density and mass flow.[78,79] Some numerical methods such as low Reynolds number κ–ω model and Reynolds stress model have been successfully adopted to predict the combined heat and mass transfer process in membrane module.

Compressed air dehumidification

Materials, structures and operation conditions

Compressed air dehumidification is another common application of membrane-based dehumidification due to less energy consumption and lower operation cost. Quite different from dehumidification under ambient pressure, compressed air dehumidification is driven by

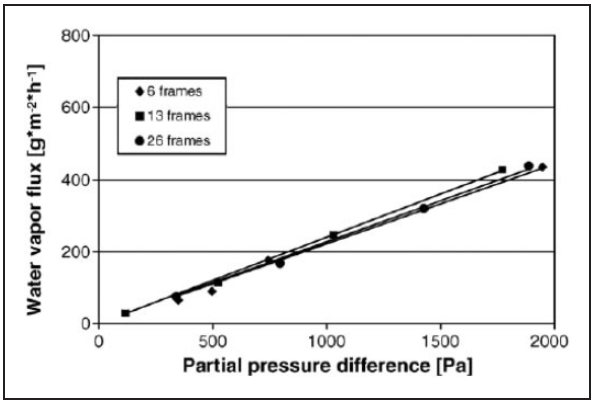

Figure 9. Water vapour flux vs. partial pressure difference at different fibre frame numbers.[80]

much larger water vapour pressure difference, so the membrane module has to be fabricated as the shell-and-tube form that can sustain high pressure.

Figure 9 presents the linear regression lines of water vapour flux versus water vapour partial pressure difference in hollow fibre membrane module experiment under various conditions of fibre frame number, alignment and diameter of the fibre frames.[80]

Therefore, mass transfer flux can be calculated by the following equation[81]

$$J = Pe\Delta pA/\delta \tag{25}$$

where Pe is water vapour permeability of the membrane (kg m m^{-2} s^{-1} Pa^{-1}) and Δp is water vapour partial pressure difference between feed and permeate (Pa).

Cactus membrane structured of hollow fibres has been successfully put into commercial operation for years.[82] In general, the higher the pressure difference is, the better dehumidification performance will be. However, air can also get through pores, and its permeation can be enhanced by increasing the pressure difference, causing production of dry air to decrease. Proper pressure difference needs to be selected, so as to balance dehumidification performance and production.

In compressed air dehumidification, there are usually two operation condition modes for carrying away water vapour. One is by vacuum and the other is by sweeping air. Sweeping air mode can effectively remove moisture on the membrane surface, by sweeping a fraction of product air back on the permeate side. The fraction has a great effect on dehumidification performance. In a compressed air dehumidification test using PI hollow fibre membrane blended with suphonated polyether-sulphone, a 30% ratio of the back-sweeping product air realized the dew point of product air as low as $-30^{\circ}C$.[83] When the fraction is greater, the concentration polarization would be weakened, at the same time the production would be reduced. Usually, these operation conditions are combined with material modification to weaken the concentration polarization so as to balance production and lower water vapour content of product air.

A support polytetrafluoroethylene membrane skinned by hydrophilic liquid triethylene glycol or polyethylene glycol 400 (PEG400) was blended with a highly hydrophobic microporous membrane.[84] Experimental investigation indicated that the moisture of feed air was successfully removed under high vacuum operation.

Some technologies to eliminate concentration polarization of hollow fibre membrane were investigated by comparing the influence of different operation conditions.[85] It was indicated that the combination of vacuum and sweeping air obtained the best dehumidification performance, and increasing sweeping air temperature favoured the removal of water vapour on the permeate side.

Compressed air from engine is a main air resource of aircraft cabin. A novel aircraft environment control system with a hollow fibre membrane dehumidifier was proposed to replace conventional high pressure de-ionized water system.[86,87] In the novel system, the humid air of high pressure was dehumidified by sweeping air through membranes first and then entered the main refrigeration turbine to be cooled down, greatly reducing the refrigeration energy needed for the removal of water vapour in high pressure air. Simulation results showed promotion by more than 70% of refrigeration capacity of the novel system compared with conventional system.

Theory models

Compressed air dehumidification is a process of composition separation of air, during which one composition flows through membrane pores faster and another one flows more slowly due to the selectivity of membrane, resulting in different permeability. Based on this mechanism, the governing equations for compressed air dehumidification are established. The counter flow process is represented by equation (26).[88]

Total mass balances

$$du = dv \tag{26}$$

Mass of water vapour balances is represented by equation (27)

$$udx + xdu = vdy + ydv \tag{27}$$

Permeate flux of water vapour is represented by equation (28)

$$JA(p_o x - p_i y)dz/L = -udx - xdu \quad (28)$$

Permeate flux of air is represented by equation (29)

$$JA[p_o(1-x) - p_i(1-y)]dz/(L\alpha) = udx - (1-x)du \quad (29)$$

Pressure drop in tubes is significant as represented by equation (30), whose influence cannot be neglected

$$dp_i/dz = 128RTK\mu v/(N\pi p_i d_i^4) \quad (30)$$

where u and v are mass flow rates (kg s^{-1}) of feed and permeate side, respectively; x and y are mass ratios of water vapour and air, respectively; J is water vapour permeability (kg s^{-1} m^{-2} Pa^{-1}); p_o and p_i are pressures (Pa) of outside and inside tubes, respectively; z is flow direction; L is tube length (m); α is separation ratio of water vapour to air; K is molar volume, 22.4 L mol^{-1}; N is tube number and d_i is inner diameter (m) of tube.

Membrane-based dehumidification for space vehicle

Humidity control in space vehicle includes passive control and active control. Passive humidity control is open-loop without feedback, independent from temperature control, which affects little on temperature in capsule. On the contrary, active humidity control is closed-loop, with humidity signals feedback. In active humidity control, humid air is first cooled to dew point then the condensate water is separated from air by gas–liquid separation process. The dehumidification capacity is controlled by regulating air flow rate. Active humidity control has become the main humidity control method in space vehicle, such as space shuttle,[89] Freedom Space Station[90] and International Space Station.[91,92] However, it is quite difficult to separate condensate water from air in microgravity.[93] It is usually done by mechanical extrusion, suction pump, rotary gas–liquid separator or absorbent material.[94] Mechanical separation process consumes more energy, while absorbent material needs to be recycled once saturated, limiting dehumidification capacity. Thus, it is critical to study a new dehumidification technology for space application.

Due to excellent reliability, light weight, small footprint, low energy consumption and combining heat and mass transfer, membrane module has been applied in thermal and humidity control of spacecraft and spacesuit.

As far back as in 1998, an application of membrane-based dehumidification by coolant water was introduced into humidity control of plant growth chamber in spacecraft.[95] Three membranes of different materials were studied comparatively: mixed cellulose ester, ceramic α-Al_2O_3 and metal 316LSS-sintered. Membrane modules were made in the form of shell-and-tube, with the humid air flowing inside tubes and the coolant water flowing outside. Cellulose has a higher porosity and a lower contact angle, gaining a better moisture transmembrane performance and the pressure drop was lower as well. Unfortunately, its durability was a little worse. The operation failed only after several days or even hours, taking the form of air bleeding through the membrane into the coolant water. Of course, the studies on membrane materials have been advancing in the passing years, and the durability problem has been resolved. As previously mentioned, the hollow fibre membrane used in compressed air dehumidification is now in commercial operation.

More recently, NASA has made abundant investigations on membrane modules applied in spacesuit. These membrane modules performed various functions, such as evaporating water vapour to vacuum to obtain cold water for liquid cooling garment,[96] removing non-condensate gas in water,[97] and releasing sensible heat and moisture produced by aspiration and metabolism.[11]

For the giant specific area, hollow fibre is the best alternative for membrane module. In an efficient module, the fibre layers were grouped into stacks which were separated by small spaces and packaged into a cylindrical shape.[96] A full-scale prototype consisted of 14,300 tube bundled into 30 stacks, each of which was formed into a chevron shape, separated by spacers and organized into three sectors of 10 nested stacks, as shown in Figure 10.

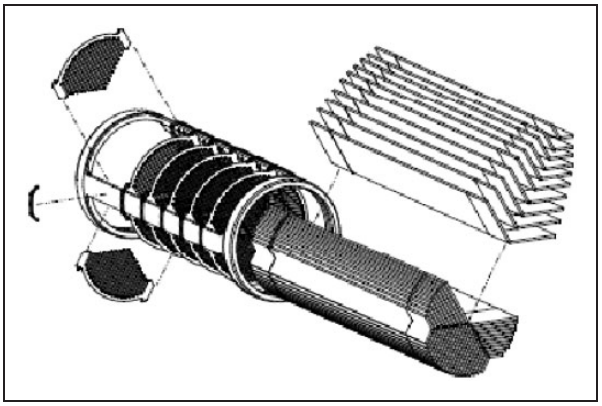

Figure 10. A hollow fibre spacesuit water membrane evaporator.[96]

A series of proof-of-concept tests for a type of non-venting spacesuit were conducted.[11] As shown in Figure 11, the porous hydrophilic pad made of non-woven wicking material was wetted by absorbing makeup water. For the lower temperature, the pad removed the sensible heat from pressure garment. Meanwhile water vapour rejected by perspiration and expiration permeated from pressure garment (about 29.6 kPa) into the vacuum pocket (2.4 kPa) made of Nafion. The moisture transferred through membrane by condensing and evaporating successively, removing the latent heat. In the end, water vapour was absorbed by LiCl desiccant, with heat rejected towards the space environment by the radiator. The proof-of-concept evaporative cooling and dehumidification garment (ECDG) could deal with 883 W/m^2 total heat load including 689 W m^{-2} latent. That meant 0.2787 m^2 of Nafion area was enough for 250 W of cooling for a spacesuit.

Membrane-based dehumidification performance evaluation

Energy analysis

The first law of thermodynamics is a common and intuitional approach to evaluate the performance of a certain thermodynamic process. Naturally, it also applies to membrane-based dehumidification.

According to heat transfer efficiency of conventional sensible heat exchanger, sensible efficiency ε_s and latent efficiency (or called dehumidification efficiency) ε_l were introduced into total heat exchanger,[37]

$$\varepsilon_s = \frac{\dot{m}_e c_{pe}(T_{eo} - T_{ei})}{(\dot{m}c_p)_{\min}(T_{fi} - T_{ei})} \tag{31}$$

$$\varepsilon_l = \frac{\dot{m}_e(\omega_{eo} - \omega_{ei})}{(\dot{m})_{\min}(\omega_{fi} - \omega_{ei})} \tag{32}$$

where subscripts '*i*' and '*o*' denote inlet and outlet, respectively; subscript '*f*' denotes fresh air, and '*e*' denotes exhaust air; $\dot{m}$ is mass flow rate (kg s^{-1}) and c_p is specific heat capacity (J kg^{-1} K^{-1}). For hot and highly humid regions, the two efficiencies are the most direct and significant factors of performance evaluation.[98]

There are some correlations of sensible and latent efficiency with respect to the total number of transfer units for sensible and latent heat (NTU_s and NUT_l).[14,99] Take a cross-flow membrane module structured of flat plates, for example

$$\varepsilon_s = 1 - \exp\left[\frac{\exp\left(-\mathrm{NTU}_s^{0.78} R_1\right) - 1}{\mathrm{NTU}_s^{-0.22} R_1}\right] \tag{33}$$

$$\varepsilon_l = 1 - \exp\left[\frac{\exp\left(-\mathrm{NTU}_l^{0.78} R_2\right) - 1}{\mathrm{NTU}_l^{-0.22} R_2}\right] \tag{34}$$

where

$$\mathrm{NTU}_s = \frac{hA}{(\dot{m}c_p)_{\min}} \tag{35}$$

$$\mathrm{NTU}_l = \frac{kA}{(\dot{m})_{\min}} \tag{36}$$

and R_1 is the ratio of minimum to maximum heat capacity rate of two fluids and R_2 is the ratio of minimum to maximum mass flow rate of two fluids.

Coupled with mass transfer process, the temperature in channels of membrane module would not change monotonically like conventional sensible heat exchanger, thus sensible efficiency may be very small under some special

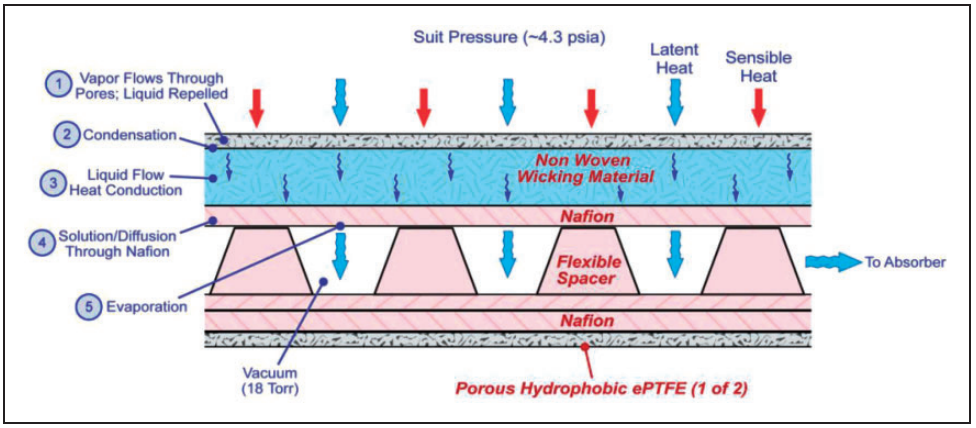

Figure 11. Cooling and water vapour absorption in the ECDG.[11]
ECDG: evaporative cooling and dehumidification garment.

operation conditions. Taking a process of air dehumidification by solution, for example, coupled with the sensible heat transferring from air to solution, water vapour permeated through membrane and was absorbed by solution, leading to the rising of solution temperature. As air temperature dropped, temperature of solution approached closely to that of air. Then the sensible efficiency drew near zero, as shown in Figure 12.[99]

Exergy analysis

Simply as an expression of the energy conservation principle, the first law considers the consumption and utilization of energy in quantity only, while the second law asserts that energy has quality as well as quantity, which comprehensively reveals the energy quality destruction occurred during the actual process. Based on this law, exergy analysis is developed to evaluate the destruction of available work.

When air is simplified as ideal gas, exergy per kilogram dry air can be gained as represented by equation (37)[100]

$$\begin{aligned} ex = {} & (c_{pa} + \omega c_{pv}) T_0 \left(\frac{T}{T_0} - 1 - \ln \frac{T}{T_0} \right) \\ & + (1 + 1.608\omega) R_a T_0 \ln \frac{p}{p_0} \\ & + R_a T_0 \left[(1 + 1.608\omega) \ln \frac{1 + 1.608\omega_0}{1 + 1.608\omega} + 1.608\omega \ln \frac{\omega}{\omega_0} \right] \end{aligned} \tag{37}$$

where subscripts 'a' and 'v' denote dry air and water vapour, respectively; subscript '0' denotes environment state. The first two terms on the right-hand side are thermal exergy and mechanical exergy, whose forms are the same with common ideal gas. The additional term is concentration exergy.

Exergy balance equation, equation (38), is established referring to indirect evaporative cooling process similarly with combination of heat and mass transfer,[101]

$$ex_{t,a} + \omega ex_{t,w} = ex_t + ex_{t,d} \tag{38}$$

where $ex_{t,d}$ is the exergy destruction of system and $ex_{t,a}$, $ex_{t,w}$ and ex_t are the exergy of dry air, moisture and humid air, respectively.

The specific exergy of water is given by equation (39)[100]

$$\begin{aligned} ex_{t,w} = {} & \left(h_{f(T_1)} - h_{g(T_0)} \right) - T_0 \left(s_{f(T_1)} - s_{g(T_0)} \right) \\ & + \left(p_1 - p_{sat(T_1)} \right) v_{f(T_1)} - R_v T_0 \ln \varphi_0 \end{aligned} \tag{39}$$

where subscripts 'f' and 'g' denote liquid and gas; subscripts '1' and '0' denote inlet state and reference state.

Thus the exergy efficiency of system is

$$\psi = \frac{\sum ex_{out}}{\sum ex_{in}} = \frac{ex_t}{ex_{t,a} + \omega ex_{t,w}} \tag{40}$$

The methods of exergy analysis above can be applied in membrane-based dehumidification process.

On the other hand, entropy analysis is also developed from the second law of thermodynamics, and has the same essence as exergy analysis. The irreversibility in membrane module was investigated from entropy perspective,[102] using the calculation given by Bejan.[100] In addition, the entropy increase per unit heat transfer amount was proposed

$$N = \frac{\Delta S_{tot}}{Q} \tag{41}$$

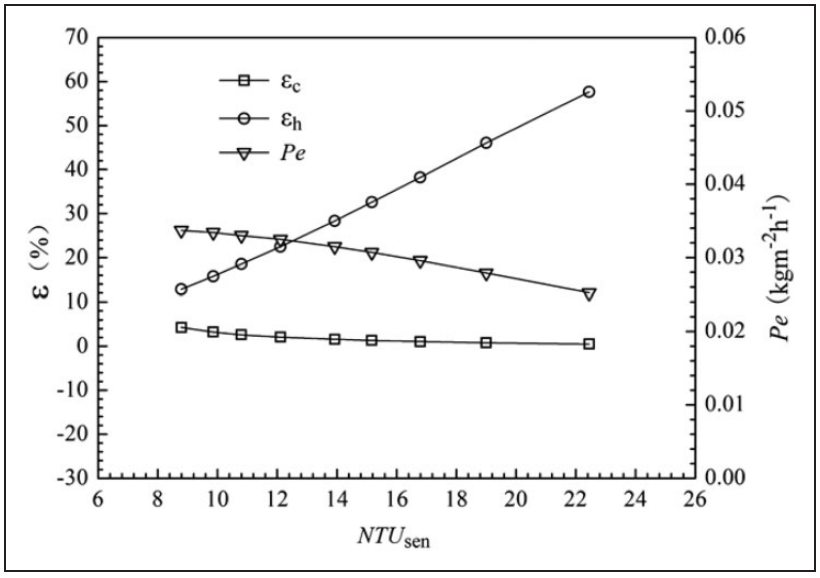

Figure 12. Sensible and latent efficiency under a certain operation condition.[99]

where ΔS_{tot} is the total entropy increase and Q is total heat transfer amount. The value of N should be low, to ensure that the entropy increase is small while the capacity of heat transfer is great at the same time.

At present, unfortunately, the selection of the reference state has not yet reached an agreement on temperature and humidity. The exergy performances of different air-conditioning systems were compared and it was found that the Maisotsenko cycle-based cooling system obtained the lowest exergy reduction when selecting 50°C as reference temperature, while those systems varied close to each other at 23° (comfortable temperature).[101] For humidity, arguments are concentrated on the dead state selection between the saturated state and the actual state of outdoor moisture air (unsaturated generally).[103]

Conclusion

As an alternative dehumidification device, membrane module can treat both sensible heat and latent heat simultaneously. It is small foot-printed, light weighted, simple structured, highly compact, and can work continuously without moving parts. Thanks to these advantages, membrane-based dehumidification technology is being gradually applied in HVAC. Additionally, it is remarkable that membrane-based dehumidification performances have great superiority over the traditional technologies especially in some special fields such as compressed air dehumidification and space vehicle environment control. With regards to different application fields, materials, structures and operation conditions can vary for a certain membrane module, on the basis of different dehumidification principles. While energy efficiency analysis is often used to evaluate dehumidification performance, exergy analysis can also be introduced by the second law of thermodynamics.

With many advantages of membrane-based dehumidification mentioned at hand, there are still some problems, including mechanical strength, thermostability, cost and so on, to be resolved yet before membrane-based dehumidification can be applied more widely in many other fields. More research work is needed on the production of new membrane material with higher mass and heat transfer performance and greater tolerance with temperature and particulate contamination.

Acknowledgement

The research on membrane-based dehumidification and moisture recovery of air was supported by the Natural Science Foundation of China (NSFC), 51176006.

References

1. Zhang HB and Hiroshi Y. Analysis of indoor humidity environment in Chinese residential buildings. *Build Environ* 2010; 45(10): 2132–2140.
2. Zhang LZ, Zhu DS, Deng XH and Hua B. Thermodynamic modeling of a novel air dehumidification system. *Energy Build* 2005; 37(3): 279–286.
3. Zhang LZ, Liang CH and Pei LX. Conjugate heat and mass transfer in membrane-formed channels in all entry regions. *Int J Heat Mass Transfer* 2010; 53(5–6): 815–824.
4. ASHRAE. Ventilation for acceptable indoor air quality. ANSI/ASHRAE Standard 62-2001. Atlanta: American Society of Heating, Refrigerating, and Air-Conditioning Engineers, Inc., 2001.
5. Liang CH, Zhang LZ and Pei LX. Performance analysis of a direct expansion air dehumidification system combined with membrane-based total heat recovery. *Energy* 2010; 35(9): 3891–3901.
6. Mahmud K, Mahmood GI, Simonson CJ and Besant RW. Performance testing of a counter-cross-flow run-around membrane energy exchanger (RAMEE) system for HVAC applications. *Energy Build* 2010; 42(7): 1139–1147.
7. Niu JL and Zhang LZ. Membrane-based enthalpy exchanger: material considerations and clarification of moisture resistance. *J Membr Sci* 2001; 189(2): 179–191.
8. Usachov VV, Teplyakov VV, Okunev AY and Laguntsov NI. Membrane contactor air conditioning system: experience and prospects. *Sep Purif Technol* 2007; 57(3): 502–506.
9. Zhang LZ and Huang SM. Coupled heat and mass transfer in a counter flow hollow fiber membrane module for air humidification. *Int J Heat Mass Transfer* 2011; 54(5–6): 1055–1063.
10. Pan FS, Jia HP, Jiang ZY, Zheng XH, Wang JT and Cui L. P(AA-AMPS)-PVA/polysulfone composite hollow fiber membranes for propylene dehumidification. *J Membr Sci* 2008; 323(2): 395–403.
11. Izenson MG, Chen WB, Phillips S and Bue G. Nonventing thermal and humidity control for EVA suits: AIAA 2011-5260, In: *41st international conference on environmental systems*, Portland, OR, USA, 17–21 July 2011.
12. Niu JL, Zhang LZ and Zuo HG. Energy savings potential of chilled-ceiling combined with desiccant cooling in hot and humid climates. *Energy* 2002; 34(5): 487–495.
13. Zhang LZ. Energy performance of independent air dehumidification systems with energy recovery measures. *Energy* 2006; 31(8–9): 1228–1242.
14. Liang CH, Zhang LZ and Pei LX. Independent air dehumidification with membrane-based total heat recovery. Modeling and experimental validation. *Refrigeration* 2010; 33(2): 398–408.
15. Bergero S and Chiari A. Performance analysis of a liquid desiccant and membrane contactor hybrid air-conditioning system. *Energy Build* 2010; 42(11): 1976–1986.
16. Yamaguchi S, Jeong J, Saito K, Miyauchi H and Harada M. Hybrid liquid desiccant air-conditioning system. Experiments and simulations. *Appl Therm Eng* 2011; 31(17–18): 3741–3747.
17. Zhang LZ. Progress on heat and moisture recovery with membranes: from fundamentals to engineering applications. *Energy Convers Manage* 2012; 63: 173–195.
18. Zhang LZ. Evaluation of moisture diffusivity in hydrophilic polymer membranes. A new approach. *J Membr Sci* 2006; 269(1–2): 75–83.
19. Wang HJ, Zhang L, Zhao SS and Wang D. Progress on vapor permeation by membrane separation technologies. *Sci Technol Inf* 2009; 36: 92–94. (in Chinese).
20. Metz SJ, Ven WJC, Potreck J, Mulder MHV and Wessling M. Transport of water vapor and inert gas mixtures through highly selective and highly permeable polymer membranes. *J Membr Sci* 2005; 251(1–2): 29–41.

21. Zhang XR, Zhang LZ, Liu HM and Pei LX. One-step fabrication and analysis of an asymmetric cellulose acetate membrane for heat and moisture recovery. *J Membr Sci* 2011; 366(1–2): 158–165.
22. Zhang XR, Zhang LZ and Pei LX. The analysis of moisture mass transfer resistance and permeability for a novel asymmetric membrane. *J Eng Thermophys* 2011; 32(8): 1382–1384. (in Chinese).
23. Zhang LZ. Fabrication of a lithium chloride solution based composite supported liquid membrane and its moisture permeation analysis. *J Membr Sci* 2006; 276(1–2): 91–100.
24. Zhang LZ and Xiao F. Simultaneous heat and moisture transfer through a composite support liquid membrane. *Int J Heat Mass Transfer* 2008; 51(9–10): 2179–2189.
25. Seshadri SK and Lin YS. Synthesis and water vapor separation properties of pure silica and aluminosilicate MCM-48 membranes. *Sep Purif Technol* 2011; 76(3): 261–267.
26. Zhang LZ, Wang YY, Wang CL and Xiang H. Synthesis and characterization of a PVA/LiCl blend membrane for air dehumidification. *J Membr Sci* 2008; 308(1–2): 198–206.
27. Zhang LZ. Numerical study of heat and mass transfer in an enthalpy exchanger with a hydrophobic-hydrophilic composite membrane core. *Numer Heat Transfer A-Appl* 2007; 51(7): 697–714.
28. Zhang LZ. A fractal model for gas permeation through porous membranes. *Int J Heat Mass Transfer* 2008; 51(21–22): 5288–5295.
29. Zhang LZ. Coupled heat and mass transfer through asymmetric porous membranes with finger-like macrovoids structure. *Int J Heat Mass Transfer* 2009; 52(3–4): 751–759.
30. Pei LX, Zhao WJ and Zhang LZ. Preparation and characterization of porous PVDF membranes for dehumidification with PEG as additive. *J Appl Polym Sci* 2010; 118(5): 2696–2703.
31. Liu HM, Zhang LZ and Pei LX. Hydrophobic modification of polyvinylidene fluride membrane. *New Chem Mater* 2011; 39(4): 80–83. (in Chinese).
32. Pei LX, Lv ZM and Zhang LZ. Selective adsorption of a novel high selective desiccant for prospective use in heat and moisture recovery for buildings. *Build Environ* 2012; 49: 124–128.
33. Zhang LZ, Zhang XR, Miao QZ and Pei LX. Selective permeation of moisture and VOCs through polymer membranes used in total heat exchangers for indoor air ventilation. *Indoor Air* 2012; 22(4): 321–330.
34. Pei LX, Zhou JR and Zhang LZ. Preparation and properties of Ag-coated activated carbon nanocomposites for indoor air quality control. *Build Environ* 2013; 63: 108–113.
35. Liu S, Riffat S, Zhao X and Yuan Y. Impact of adsorbent finishing and absorbent filming on energy exchange efficiency of an air-to-air cellulose fibre heat & mass exchanger. *Build Environ* 2009; 44(9): 1803–1809.
36. Lipnizki F and Field RW. Mass transfer performance for hollow fibre modules with shell-side axial feed flow: using an engineering approach to develop a framework. *J Membr Sci* 2001; 193(2): 195–208.
37. Zhang LZ. An analytical solution for heat mass transfer in a hollow fiber membrane based air-to-air heat mass exchanger. *J Membr Sci* 2010; 360(1): 217–225.
38. Defraeye T, Blocken B and Carmelier J. Analysis of convective heat and mass transfer coefficients for convective drying of a porous flat plate by conjugate modelling. *Int J Heat Mass Transfer* 2012; 55(1–3): 112–124.
39. Zhang LZ, Liang CH and Pei LX. Heat and moisture transfer in application scale parallel-plates enthalpy exchangers with novel membrane materials. *J Membr Sci* 2008; 325(2): 672–682.
40. Zhang LZ. An analytical solution to heat and mass transfer in hollow fiber membrane contactors for liquid desiccant air dehumidification. *J Heat Transfer-T ASME* 2011; 133(9): 2001–2008.
41. Zhang LZ and Li ZX. Convective mass transfer and pressure drop correlations for cross-flow structured hollow fiber membrane bundles under low Reynolds numbers but with turbulent flow behaviors. *J Membr Sci* 2013; 434: 65–73.
42. Zhang LZ. Coupled heat and mass transfer in an application-scale cross-flow hollow fiber membrane module for air humidification. *Int J Heat Mass Transfer* 2012; 55(21–22): 5861–5869.
43. Zhang LZ. Heat and mass transfer in a quasi-counter flow membrane-based total heat exchanger. *Int J Heat Mass Transfer* 2010; 53(23–24): 5478–5486.
44. Zhang LZ. Heat and mass transfer in a cross-flow membrane-based enthalpy exchanger under naturally formed boundary conditions. *Int J Heat Mass Transfer* 2007; 50(1–2): 151–162.
45. Zhang LZ. Laminar flow and heat transfer in plate-fin triangular ducts in thermally developing entry region. *Int J Heat Mass Transfer* 2007; 50(7–8): 1637–1640.
46. Zhang LZ. Thermally developing forced convection and heat transfer in rectangular plate-fin passages under uniform plate temperature. *Numer Heat Transfer A-Appl* 2007; 52(6): 549–564.
47. Zhang LZ. Heat and mass transfer in plate-fin sinusoidal passages with vapor-permeable wall materials. *Int J Heat Mass Transfer* 2008; 51(3–4): 618–629.
48. Zhang LZ. Heat and mass transfer in plate-fin enthalpy exchangers with different plate and fin materials. *Int J Heat Mass Transfer* 2009; 52(11–12): 2704–2713.
49. Vali A. *Modeling a run-around heat and moisture exchanger using two counter/cross flow exchangers*. MSc Thesis, Department of Mechanical Engineering University of Saskatchewan, Saskatchewan, Canada, 2009.
50. Zhang LZ. Convective mass transport in cross-corrugated membrane exchangers. *J Membr Sci* 2005; 260(1–2): 75–83.
51. Zhang LZ. Heat and mass transfer in a total heat exchanger: cross-corrugated triangular ducts with composite supported liquid membrane. *Numer Heat Transfer A-Appl* 2008; 53(11): 1195–1210.
52. Scott K and Lobato J. Mass transfer characteristics of cross-corrugated membranes. *Desalination* 2002; 146(1–3): 255–258.
53. Zhang LZ and Chen ZY. Convective heat transfer in cross-corrugated triangular ducts under uniform heat flux boundary conditions. *Int J Heat Mass Transfer* 2011; 54(1–3): 597–605.
54. Zhang LZ. Numerical study of periodically fully developed flow and heat transfer in cross-corrugated triangular channels in transitional flow regime. *Numer Heat Transfer A–Appl* 2005; 48(4): 387–405.
55. Zhang LZ. Turbulent three-dimensional air flow and heat transfer in a cross-corrugated triangular duct. *J Heat Transfer-T ASME* 2005; 127(10): 1151–1158.
56. Zhang LZ. Performance deteriorations from flow maldistribution in air-to-air heat exchangers: a parallel-plates membrane core case. *Numer Heat Transfer A-Appl* 2009; 56(9): 746–763.
57. Zhang LZ. Flow maldistribution and thermal performance deterioration in a cross-flow air to air heat exchanger with plate-fin cores. *Int J Heat Mass Transfer* 2009; 52(19–20): 4500–4509.
58. Zhang LZ. Flow maldistribution and performance deteriorations in membrane-based heat and mass exchangers. *J Heat Transfer-T ASME* 2009; 131(11): 1118011-7.
59. Zhang LZ. Heat and mass transfer in a randomly packed hollow fiber membrane module: a fractal model approach. *Int J Heat Mass Transfer* 2011; 54(13–14): 2921–2931.
60. Zhang LZ, Li ZX, Zhong TS and Pei LX. Flow maldistribution and performance deteriorations in a cross flow hollow fiber membrane module for air humidification. *J Membr Sci* 2013; 427: 1–9.
61. Isetti C, Nannei E and Magrini A. On the application of a membrane air-liquid contactor for air dehumidification. *Energy Build* 1997; 25(3): 185–193.
62. Bergero S and Chiari A. Experimental and theoretical analysis of air humidification or dehumidification processes using hydrophobic capillary contactor. *Appl Therm Eng* 2001; 21(11): 1119–1135.

63. He GH, Mi YL, Yue PL and Chen GH. Theoretical study on concentration polarization in gas separation membrane processes. *J Membr Sci* 1999; 153(2): 243–258.
64. Bui VA, Vu LTT and Nguyen MH. Modelling the simultaneous heat and mass transfer of direct contact membrane distillation in hollow fibre modules. *J Membr Sci* 2010; 353(1–2): 85–93.
65. Karlsson HOE and Tragardh G. Heat transfer in pervaporation. *J Membr Sci* 1996; 119(2): 295–306.
66. Thomas LC. *Heat transfer*. Englewood Cliffs, NJ: Prentice Hall, 1992.
67. Prasad P and Sirkar KK. Dispersion-free solvent extraction with microporous hollow-fiber modules. *AIChE J* 1998; 34(2): 177–188.
68. Costello MJ, Fane AG, Hogan PA and Schofield RW. The Effect of shell side hydrodynamics on the performance of axial flow hollow fibre modules. *J Membr Sci* 1993; 80(1): 1–11.
69. Viegas RMC, Rodriguez M, Luque S, Alvarez JR, Coelhoso IM and Crespo JPSG. Mass transfer correlations in membrane extraction: analysis of Wilson-plot methodology. *J Membr Sci* 1998; 145(1): 129–142.
70. Wu J and Chen V. Shell-side mass transfer performance of randomly packed hollow fiber modules. *J Membr Sci* 2000; 172(1–2): 59–74.
71. Juang RS, Lin SH and Yang MC. Mass transfer analysis on air stripping of VOCs from water in microporous hollow fibers. *J Membr Sci* 2005; 255(1–2): 79–87.
72. Min JC, Hu T and Song YZ. Experimental and numerical investigations of moisture permeation through membranes. *J Membr Sci* 2011; 367(1–2): 174–181.
73. Zhang LZ. Mass diffusion in a hydrophobic membrane humidification/dehumidification process: the effects of membrane characteristics. *Sep Sci Technol* 2006; 41(8): 1565–1582.
74. Zhang LZ. Investigation of moisture transfer effectiveness through a hydrophilic polymer membrane with a field and laboratory emission cell. *Int J Heat Mass Transfer* 2006; 49(5–6): 1176–1184.
75. Zhang LZ. Effects of membrane parameters on performance of vapor permeation through a composite supported liquid membrane. *Sep Sci Technol* 2006; 41(16): 3517–3538.
76. Huang SM, Zhang LZ, Tang K and Pei LX. Fluid flow and heat mass transfer in membrane parallel-plates channels used for liquid desiccant air dehumidification. *Int J Heat Mass Transfer* 2012; 55(9–10): 2571–2580.
77. Zhang LZ, Huang SM, Chi JH and Pei LX. Conjugate heat and mass transfer in a hollow fiber membrane module for liquid desiccant air dehumidification: a free surface model approach. *Int J Heat Mass Transfer* 2012; 55(13–14): 3789–3799.
78. Zhang LZ, Huang SM and Pei LX. Conjugate heat and mass transfer in a cross-flow hollow fiber membrane contactor for liquid desiccant air dehumidification. *Int J Heat Mass Transfer* 2012; 55(25–26): 8061–8072.
79. Huang SM, Zhang LZ, Tang K and Pei LX. Turbulent heat and mass transfer across a hollow fiber membrane tube bank in liquid desiccant air dehumidification. *J Heat Transfer-T ASME* 2012; 134(8): 082001-1-10.
80. Kneifel K, Nowak S, Albrecht W, Hilke R, Just R and Peinemann KV. Hollow fiber membrane contactor for air humidity control: Modules and membranes. *J Membr Sci* 2006; 276(1–2): 241–251.
81. Sijbesma H, Nymeijer K, van Marwijk R, Heijboer R, Potreck J and Wessling M. Flue gas dehydration using polymer membranes. *J Membr Sci* 2008; 313(1–2): 263–276.
82. Yan WC. A novel air dehumidification technology based on Cactus membrane. *Chem Eng Oil Gas* 2001; 30(6): 282–286. [in Chinese].
83. Wu YL, Peng X, Liu JZ, Kong QY, Shi BL and Tong MS. Study on the integrated membrane processes of dehumidification of compressed air and vapor permeation processes. *J Membr Sci* 2002; 196(2): 179–183.
84. Ito A. Dehumidification of air by a hygroscopic liquid membrane supported on surface of a hydrophobic microporous membrane. *J Membr Sci* 2000; 175(1): 35–42.
85. Li GM, Li JF, Liu JZ and Wu YL. Water vapor permeation and air dehydration properties of modified polyimide membranes. *J East China Univ Sci Technol (Natural Sci Edn)* 2006; 32(6): 629–633. [in Chinese].
86. Yuan WX, Wang CJ and Li YX. Simulation study of an original membrane-based dehumidification aircraft environmental control system. *Acta Aeronautica et Astronautica Sinica* 2011; 32(4): 589–597. [in Chinese].
87. Yuan WX, Li YX and Wang CJ. Comparison study of membrane dehumidification aircraft environmental control system. *J Aircraft* 2012; 49(3): 815–821.
88. He GH, Xu RX and Zhu BL. Mathematic model of hollow fiber membrane gas separator. *J Chem Ind Eng (China)* 1994; 45(2): 162–167. [in Chinese].
89. Bond TA, Metcalf JT and Ascuncion C. Shuttle obiter active thermal control subsystem design and flight experience: SAE 911966. In: *21st international conference on environmental systems*, San Francisco, CA, USA, 1 July 1991.
90. Wegrich RD. Space station freedom thermal control and life support system design: *IAF-92-0691*, In: *43rd Congress of the international astronautical federation*, Washington DC, USA, August 28–September 5 1992.
91. Mascellani E, Pavarani A, Vaccaneo P, Szigetvari Z and Persson J. Columbus active thermal control equipment development. SAE 2005-01-2769, 2005.
92. Bockstahler K, Westermann H and Witt J. Advanced stainless steel condensing heat exchanger. SAE 2005-01-2805, 2005.
93. Ray R, Newbold DD, McCray SB, Friesen DT and Kliss M. A novel membrane device for the removal of water vapor and water droplets from air. SAE 921322, 1992.
94. Newbold DD, McCray SB, Millard DL and Ray R. Performance of a membrane-based condensate-recovery heat exchanger. SAE 961356, 1996.
95. Scovazzo P, Burgos J, Hoehn A and Todd P. Hydrophilic membrane-based humidity control. *J Membr Sci* 1998; 149(1): 69–81.
96. Bue GC, Makinen J, Vogel M, Honas M, Dillon P, Aaron, Colunga, Truong L and Porwitz D. Hollow fiber flight prototype spacesuit water membrane evaporator design and testing: AIAA 2011-5259. In: *41st International conference on environmental systems*, Portland, OR, USA, 17–21 July 2011.
97. Weng DC, Bowman B, Fietkiewicz B: Hydrophobic hollow fiber module for non-condensable gases removal and heat rejection: AIAA 2010-8674, AIAA SPACE 2010 Conference & Exposition, 30 August–2 September 2010, Anaheim, California, United States.
98. Zhang LZ and Niu JL. Energy requirements for conditioning fresh air and the long-term savings with a membrane-based energy recovery ventilator in Hong Kong. *Energy* 2001; 26(2): 119–135.
99. Zhang LZ and Niu JL. Effectiveness correlations for heat and moisture transfer processes in an enthalpy exchanger with membrane cores. *J Heat Transfer-T ASME* 2002; 124(5): 922–929.
100. Bejan A. *Advanced engineering thermodynamics*. New York: John Wiley & Sons, 1988.
101. Caliskan H, Dincer I and Hepbasli A. Exergetic and sustainability performance comparison of novel and conventional air cooling systems for building applications. *Energy Build* 2011; 43(6): 1461–1472.
102. Zhang MR, Zhang LZ and Xu XL. Entropy analysis of membrane-based heat and mass exchanger. *J Chem Ind Eng (China)* 2005; 56(11): 2069–2072. (in Chinese).
103. Cammarata G, Fichera A, Mammino L and Marletta L. Exergonomic optimization of an air conditioning system. *J Energy Resour* 1997; 119(1): 62–69.